Title	Single Cyclized Molecule Versus Single Branched Molecule: A Simple and Efficient 3D "Knot" Polymer Structure for Nonviral Gene Delivery
Author(s)	Newland, Ben; Zheng, Yu; Jin, Yao; Abu-Rub, Mohammad; Cao, Hongliang; Wang, Wenxin; Pandit, Abhay
Publication Date	2012-02-12
Publication Information	Newland, B,Zheng, Y,Jin, Y,Abu-Rub, M,Cao, HL,Wang, WX,Pandit, A (2012) 'Single Cyclized Molecule Versus Single Branched Molecule: A Simple and Efficient 3D Knot Polymer Structure for Nonviral Gene Delivery'. Journal Of The American Chemical Society, 134 :4782-4789.
Publisher	American Chemical Society
Link to publisher's version	http://dx.doi.org/10.1021/ja2105575
Item record	http://hdl.handle.net/10379/3002
DOI	http://dx.doi.org/DOI 10.1021/ja2105575

JACS
JOURNAL OF THE AMERICAN CHEMICAL SOCIETY

Article

pubs.acs.org/JACS

Single Cyclized Molecule Versus Single Branched Molecule: A Simple and Efficient 3D "Knot" Polymer Structure for Nonviral Gene Delivery

Ben Newland,[‡] Yu Zheng,[‡] Yao Jin, Mohammad Abu-Rub, Hongliang Cao, Wenxin Wang,* and Abhay Pandit*

Network of Excellence for Functional Biomaterials, National University of Ireland, Galway, Ireland

Supporting Information

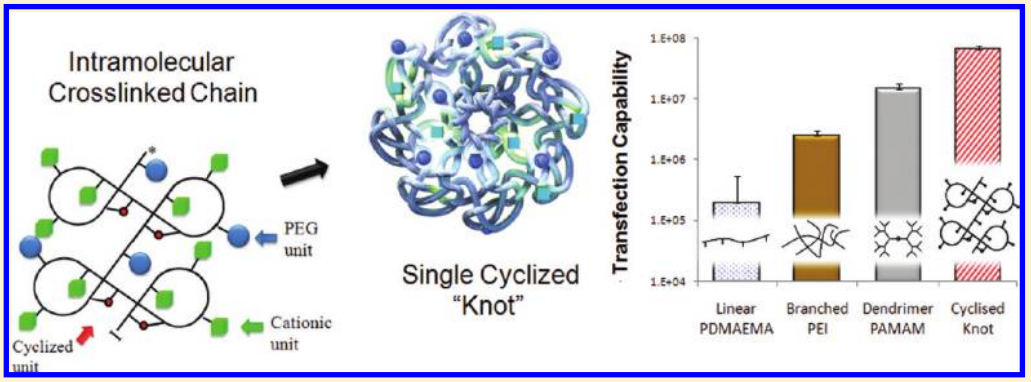

ABSTRACT: The large research effort focused on enhancing nonviral transfection vectors has clearly demonstrated that their macromolecular structure has a significant effect on their transfection efficacy. The 3D branched polymeric structures, such as dendrimers, have proved to be a very effective structure for polymeric transfection vectors; however, so far the dendritic polymers have not delivered on their promise. This is largely because a wide range of dendritic polymer materials with tailored multifunctional properties and biocompatibility required for such applications are not yet accessible by current routes. Herein, we report the design and synthesis of new 3D "Single Cyclized" polymeric gene vectors with well-defined compositions and functionalities via a one-step synthesis from readily available vinyl monomers. We observe that this polymer structure of a single chain linked to itself interacts differently with plasmid DNA compared to conventional vectors and when tested over a range of cell types, has a superior transfection profile in terms of both luciferase transfection capability and preservation of cell viability. This new knotted structure shows high potential for gene delivery applications through a combination of simplicity in synthesis, scalability, and high performance.

INTRODUCTION

The continuous identification of disease causing gene abnormalities and potential therapeutic nucleic acids inspires ever-increasing interest in genetic-based therapies for a wide range of diseases. However, the effective delivery remains one of the limiting factors despite much research focused on improvement of the vector. For true realization of genetic therapies on a large scale, vectors must be considered not only in terms of safety and efficacy, but also in terms of cost and scalability. While viral vectors are largely considered to be the most effective method of gene delivery, safety concerns and difficulty in scale-up continue as potential constraints to viral mediated gene therapies.[1,2] Thus, the design and synthesis of nonviral vectors with well-defined compositions, architectures, and functionalities that promote transfection is a challenging task in materials science.[3−5] Since the polyamidoamine dendrimer (PAMAM) demonstrated that its 3D hyperbranched structure could facilitate effective transfection,[6] much effort has been directed toward the preparation of branched versions of common transfection agents, for example, polyethylenimine (PEI),[7−9] poly-L-lysine (PLL),[10] and poly(2-(dimethylaminoethyl) methacrylate) (PDMAEMA).[11−13] These developments show that a higher transfection performance can often be achieved, highlighting potential benefits of branched structures.

Previously we have reported a deactivation enhanced atom transfer polymerization (DE-ATRP) approach, which can suppress the gelation and produce "hyperbranched" polymers from the homopolymerization of multivinyl monomers (MVMs).[14] On the basis of this deactivation enhanced strategy, a "hyperbranched" transfection agent, which used a high proportion of ethylene glycol dimethacrylate (EGDMA) as a branching agent, was designed and prepared via in situ deactivation enhanced atom transfer radical polymerization (in situ DE-ATRP).[15] However, some of the experimental results are puzzling, the most pronounced of which was the low PDI of the polymers (<2), but with a high degree of branching, certainly not the hallmark feature of hyperbranched structures.

Received: November 17, 2011
Published: February 21, 2012

   dx.doi.org/10.1021/ja2105575 | J. Am. Chem. Soc. 2012, 134, 4782−4789

Scheme 1. Illustration of the In Situ DE-ATRP Reaction Alongside a Graphical Representation of the Formation of the Cyclized Knot Structure[a]

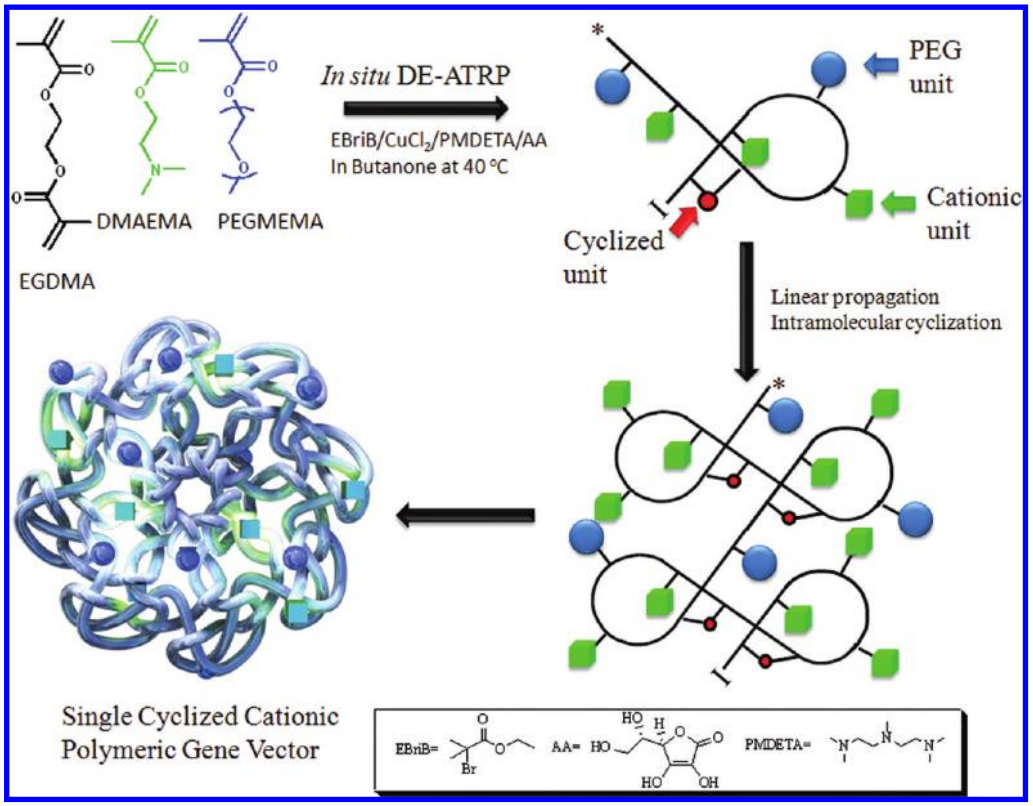

[a]Propagation and intramolecular cross-linking events (cyclization) predominantly occur throughout the reaction process forming a condensed structure consisting of single cyclized chains.

It is well-known that by the conventional statistical theory defined by Flory and Stockmayer (F−S theory) and the commonplace experimental evidence of vinyl addition polymerization, such a type of synthesis should not be possible, as only a small inclusion of multivinyl monomers should lead to the formation of insoluble cross-linked gel even at very low conversion.[16−21] We now realize that in situ DE-ATRP provides not only better control over the molecular weight and polydispersity (PDI), but also the potential to kinetically control the molecular architecture in the polymerization of MVMs. Therefore, a new polymer architecture was being formed which predominantly consists of internal cyclization reactions, i.e., intramolecular cyclization within a polymer chain rather than the usual hyperbranching between polymer chains (intermolecular cross-linking). This newly fathomed polymer architecture—single chains knotted upon themselves, is termed a "single cyclized" molecular structure,[22] in contrast to the "single branched" structure of dendrimers. As numerous reports in literature demonstrate that a higher transfection performance can be achieved through the branched architecture, it can be reasonably hypothesized that the new knotted structure of single cyclized polymer chains will out-perform currently available polymer structures in terms of efficacy, cell viability, and scalability.

Herein, we report the use of this new structure for gene delivery applications through the preparation of a series of cationic single cyclized transfection agents by the copolymerization of EGDMA (cyclizing unit), DMAEMA (cationic unit), and polyethylene glycol methyl ether methylacrylate (PEGMEMA) via in situ DE-ATRP. As previously demonstrated, in situ DE-ATRP can be used to efficiently delay the point of gelation with 60% monomer conversion in the homopolymerization of EGDMA under a concentrated polymerization condition, which led to the formation a 3D "single cyclized" polymer architecture.[22] A new kinetic model to supplement F−S theory was then introduced to explain both the ability to kinetically control the macromolecular structure and the occurrence of intramolecular reactions. This model allowed us to predict that the deactivation enhanced strategy could, in principle, be applied to the copolymerization system of MVMs. Therefore, based on this new kinetic model, in situ DE-ATRP coupled with a high monomer to initiator ratio (1000 to 1) is employed with the rationale that by ensuring high cyclization but eliminating intermolecular cross-linking, a knotted structure for high transfection efficacy can be achieved (Scheme 1). The logic for hypothesizing this structure will lead to greater performance is 2-fold: first, by the elimination of intermolecular cross-linking, a polymer of much lower PDI can be achieved and, second, by the creation of a 3D structure for DNA interaction.

The aim is therefore to assess if the cyclic knot vector can supersede the dendritic structure in terms of both transfection capability and lower toxicity. Here, a well-known commercially available dendrimer transfection vector (a partially degraded PAMAM dendrimer, SuperFect) is used as a comparable sample. Dendrimer synthesis is a time-consuming and costly process, so we demonstrate the ease of modifying the knot polymer in situ. The new cyclic polymers with varying molecular weights and degrees of polyethylene glycol content (both well-known to affect the performance of transfection)

dx.doi.org/10.1021/ja2105575 | J. Am. Chem. Soc. 2012, 134, 4782−4789

Table 1. The Composition of the Cyclic Knot Polymers Can Be Varied by Adjusting the Monomer Feed Ratios of This Simple "One-Pot" Reaction, with Very Low Final PDI Values Even at High Conversions

	monomer feed ratios						
polymer	DMAEMA	PEGMEMA	EGDMA	M_n (kDa)	M_w (kDa)	PDI	conversion (%)
PD-E 0%PEG	350	0	50	14.2	19.1	1.35	68
PD-E 8%PEG	820	80	100	21.0	32.4	1.54	38
PD-E 14%PEG	760	140	100	21.8	37.4	1.70	56
PD-E 20%PEG	700	200	100	17.5	24.8	1.42	31

were synthesized. Finally, two of these polymers were studied over a range of cell types including primary cells and stem cells, showing that the knot structure is superior to the PAMAM dendrimer for many potential applications.

RESULTS AND DISCUSSION

Polymer Synthesis and Characterization. We have recently discovered that it is no longer a formidable task to homopolymerize MVMs by controlled/living radical polymerization based on our so-termed "deactivation enhanced strategy". We have also introduced a new kinetic model to supplement F−S theory, termed the "Kinetic Theory",[22] which can be used to explain the ability to kinetically control the homopolymerization of EGDMA and the occurrence of intramolecular cyclization reactions. This theory brings the spatial proximity of reactants into consideration, allowing the prediction of conditions where the internal cyclization can occur. One such condition is when the instantaneous growth boundary is vastly reduced, such as during in situ DE-ATRP, which suppresses intermolecular cross-linking without requiring highly dilute conditions. This theory is extended here to the copolymerization of MVMs so that even in a concentrated reaction and with a high proportion of branching agent, predominately propagation/intramolecular cyclization reactions occur. Scheme 1 outlines the design and synthesis of the knot polymers, which by varying the monomer feed ratios allow for a range of degrees of PEGylation, described in Table 1. The reaction process was followed by GPC analysis of samples extracted during the reaction. Figure S1 in the Supporting Information (SI) shows typical GPC traces for the knot polymer synthesis, illustrating the controlled nature of growth by highly symmetrical and narrow peaks, the first tell-tale sign of a predominantly internal-cyclized polymer structure. Figure S1 (Supporting Information (insert)) shows that the PDI increases with increasing monomer conversion, but at a rate far lower than would be expected for typical hyperbranched polymers.[23,24]

Determination of the polymer structure by analysis of the ^{1}H NMR spectroscopy shows that these polymers do indeed have a high degree of "branching", i.e., internal cyclization (45% of the multivinyl EGDMA monomer, see SI eq S1 and SI Table S1). It also leaves free vinyl groups within the polymer structure (11%) providing an opportunity for a host of postsynthesis functionalizations. To confirm the presence of a knotted architecture, a branching monomer that can be broken upon reduction was used as a substitute for EGDMA in the PD-E 8% PEG polymer, and the degradation profile was observed. A disulfide dimethacrylate (DSDMA)[25] was used for this purpose, which undergoes fast reduction upon the addition of 20 mM glutathione (Figure 1a). If a typical hyperbranched structure was being formed, exposing the polymer to glutathione would result in cleavage of the branching units, including those used as intermolecular links, resulting in smaller fragments of polymer being produced. However, if a knotted polymer undergoes reduction by glutathione, only intramolecular cross-links are broken. Figure 1b shows schematically that this would result in a change in the polymer structure but not a significant reduction in hydrodynamic volume and molecular weight, as generally smaller fragments are not broken off. So this disulfide version of PD-E 8%PEG was analyzed for its M_w and PDI before and after being subjected to 1 h of glutathione treatment. Only a slight reduction in M_w occurred (Figure 1c), confirming that this structure is comprised predominantly of single cyclized chains.

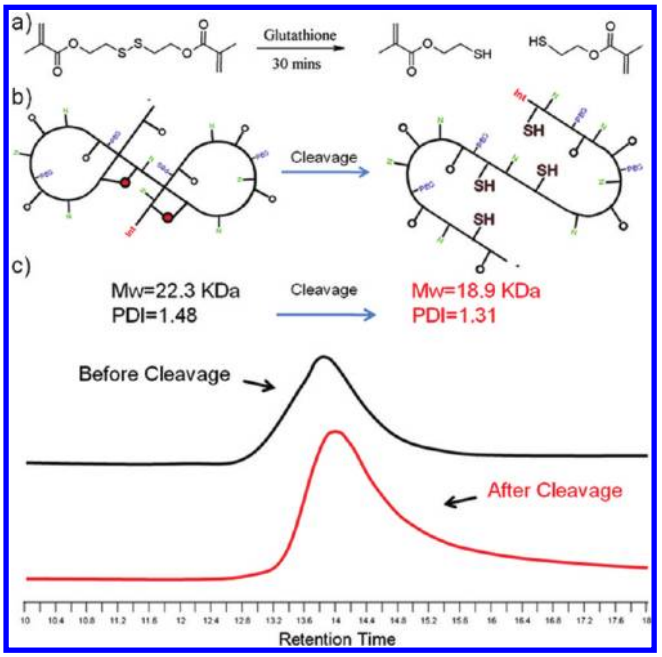

Figure 1. Evidence for the knot structure was provided by replacement of EGDMA with the disulfide monomer DSDMA (a), which can be reduced quickly in 20 mM glutathione. Part b shows schematically how the cleavage of this monomer within the polymer structure would not lead to small polymer fragments, as a typically branched polymer would. GPC data (c) show little effect on M_w after cleavage of the disulfide bond.

Buffering Capability. The first stage of analysis of these polymers for use as a transfection agent involved observing their buffering capability. Although prior studies have shown conflicting evidence,[26] endosomal escape by polymer buffering followed by endosome swelling and lysis can be regarded as one of the many routes to endosomal escape,[27] a limiting step in the transfection process. Both PD-E 8%PEG and PD-E 14%PEG buffered well against HCl between pH 7.5 and 5.5 (SI Figure S2), with no difference between them as there is only a 6% decrease in the amine containing DMAEMA by feed ratio.

Polymer/DNA Interaction. The polymer/DNA interaction (polyplex) characterization was performed by a series of

dx.doi.org/10.1021/ja2105575 | J. Am. Chem. Soc. 2012, 134, 4782−4789

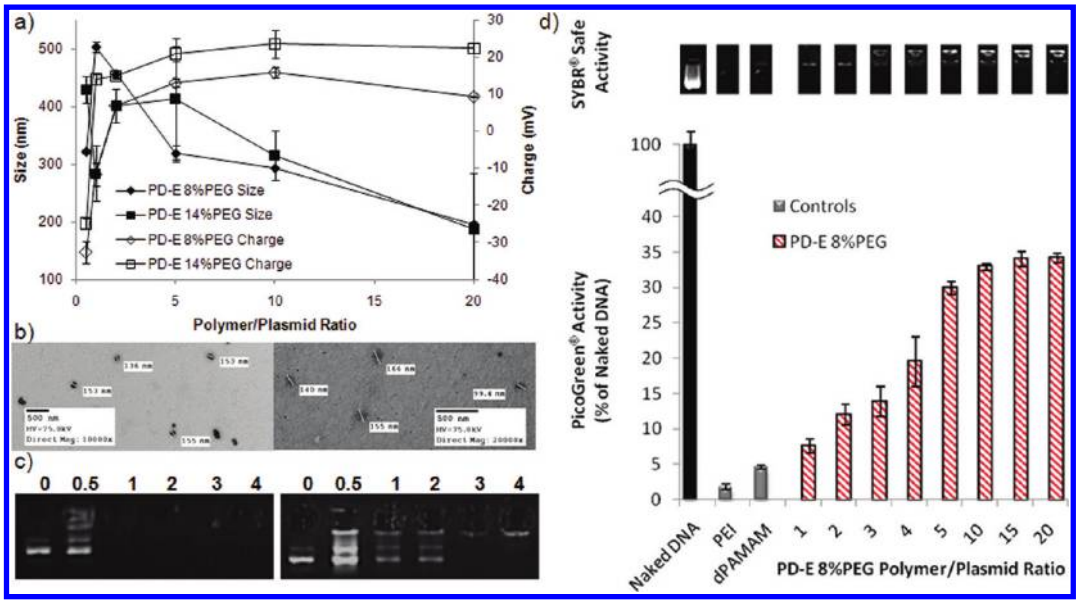

Figure 2. The hydrodynamic diameter for PD-E 8%PEG and PD-E 14%PEG polymers at a plasmid/polymer ratio (w/w) of 5:1 is in the region of ~300−400 nm by size/charge analysis (a). Part b shows dried samples of the 5:1 ratio (w/w) polyplexes of PD-E 8%PEG (left) and PD-E 14%PEG (right) to be smaller as expected, and gel electrophoresis (c) shows that PD-E 8%PEG (left) complexes DNA at a ratio of 1:1 (w/w) and that PD-E 14%PEG (right) complexes well at a 3:1 ratio (w/w). Part d shows clearly a difference in polyplex formation between the commercially available transfection agents and the cyclic knot structure, via a substantial change in the ability of dyes to intercalate with the complexed DNA in PD-E 8% PEG polyplexes (n = 3, error bars indicate ± standard deviation).

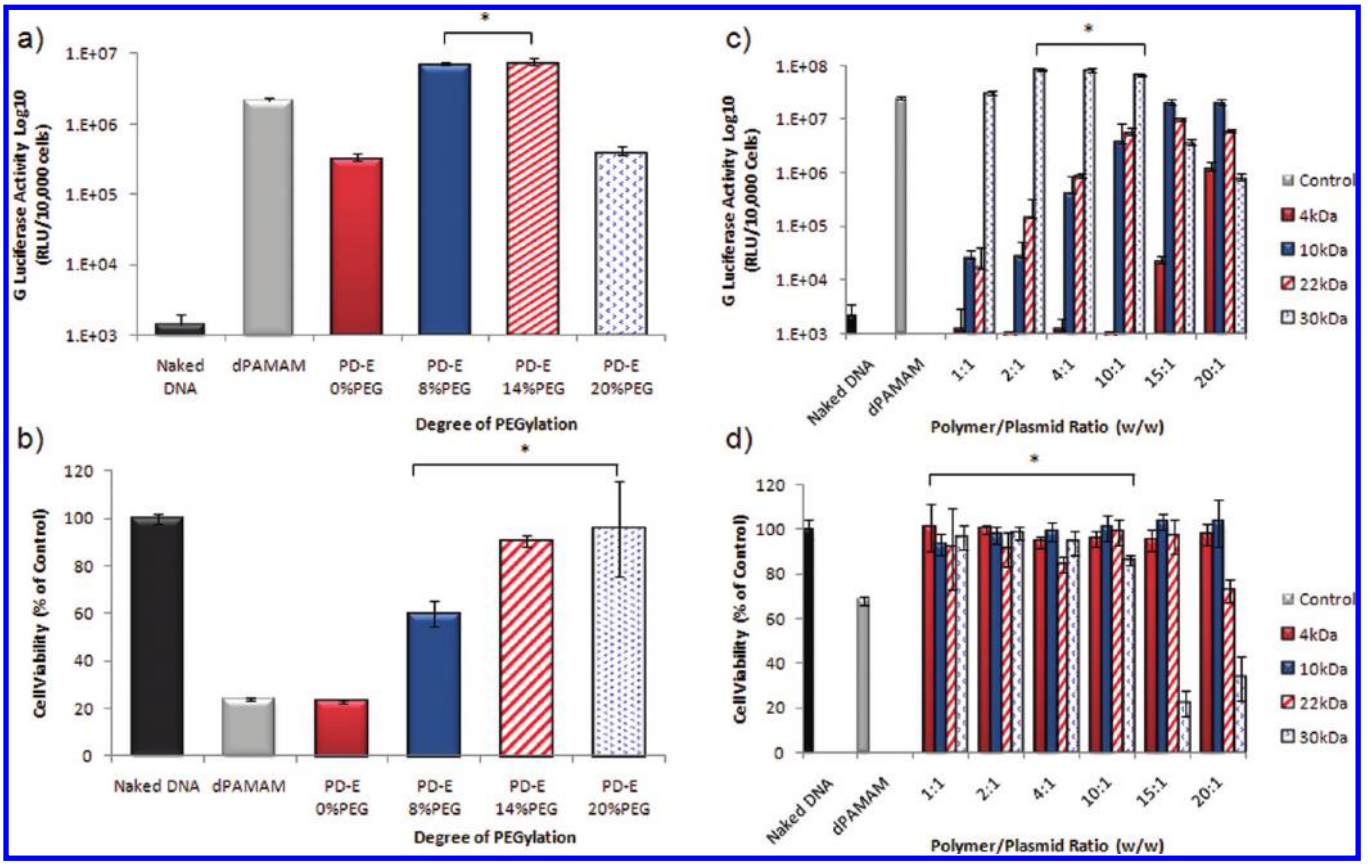

Figure 3. Increasing the degree of PEGylation affects the transfection capability of the cyclic knot polymer (a), and has a direct effect on reducing cytotoxicity (3T3 cells) (b). Four molecular weights of PD-E 8%PEG showed to have varying transfection properties with a general trend toward increasing molecular weight yielding higher transfection (c) but increased cytotoxicity (HeLa cells) (d) (for all panels: n = 4, 10 000 cells and 1 μg of pDNA per well, error bars indicate ± standard deviation and asterisks indicate significant differences from dPAMAM).

methods which allowed determination of the size of the polyplex hydrated (by dynamic light scattering, Figure 2a) and dried (TEM, Figure 2b). As with PAMAM structures, PD-E 8% PEG and PD-E 14%PEG both showed smaller diameters when

dx.doi.org/10.1021/ja2105575 | J. Am. Chem. Soc. 2012, 134, 4782−4789

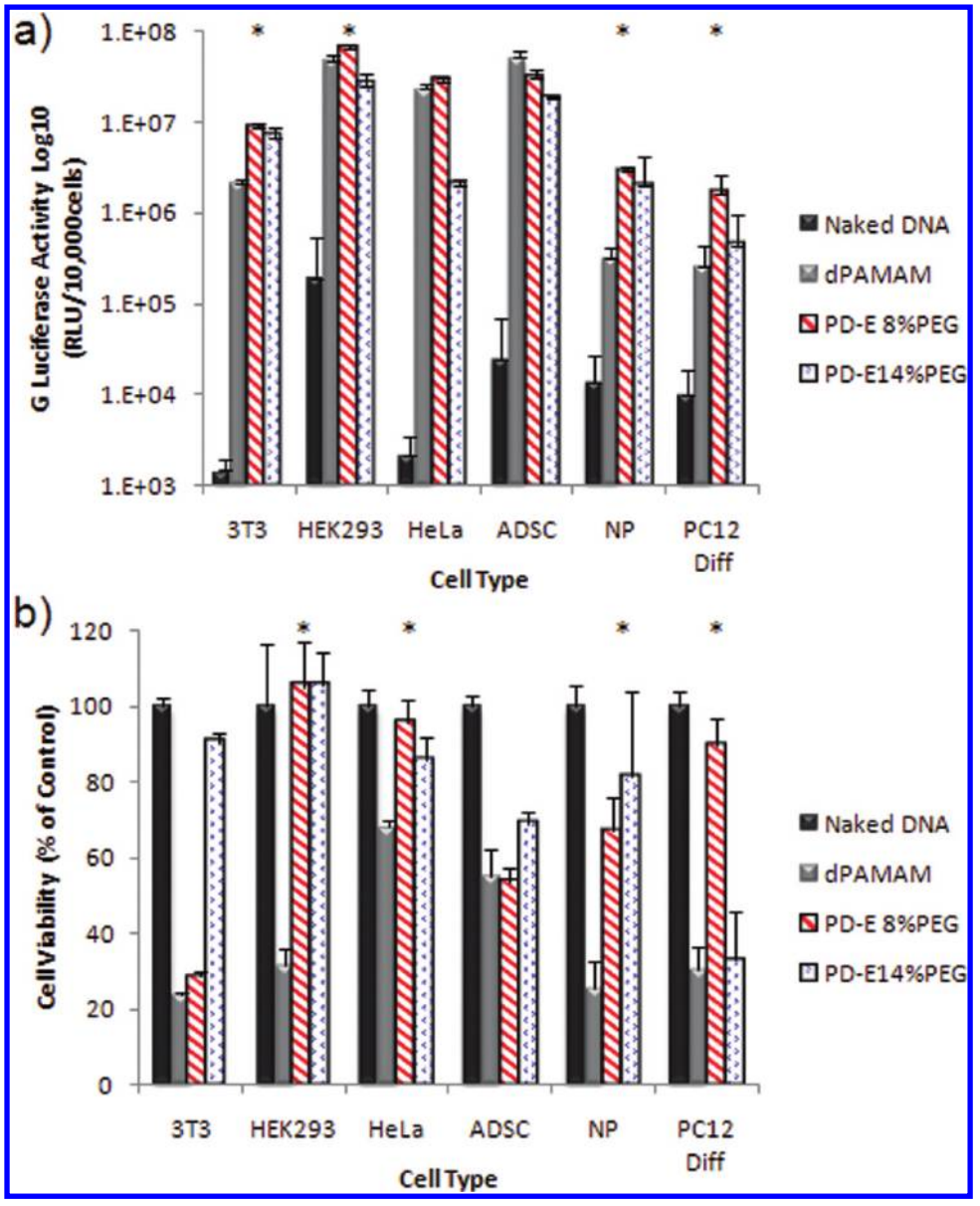

Figure 4. Over a range of immortalized cell lines, stem cells, primary cells, and neuron cells the PD-E 8%PEG polymer shows to have more favorable transfection properties in terms of transfection ability (a) and cytotoxicity (b) than the SuperFect PAMAM dendrimer (n = 4, 10 000 cells and 1 μg of pDNA per well, error bars indicate ± standard deviation, and asterisks indicate a significant difference from dPAMAM).

dry (~150 nm) than when hydrated (~300–400 nm).[28] It is important to note that small discrepancies may also occur as these studies used polyplexes formed in water (deemed appropriate for DLS measurements), as opposed to serum free media for subsequent studies. Figure 2c shows PD-E 8% PEG to have the ability to successfully complex DNA at a 1:1 weight/weight ratio; however, PD-E 14%PEG showed complexation at a 3:1 polymer/plasmid w/w ratio as it contains a higher weight fraction of neutral PEG. Interestingly, it appears that when PEI and dPAMAM form complexes, there is no fluorescence observed from the SYBR Safe DNA stain in the wells where they are held. However, a glow in the wells of the knot polymers was noticed that was augmented at higher weight ratios (Figure 2d). This change in fluorescence indicates that there is a difference in the interaction between the knot polymers and conventional branched polymers in terms of the condensation of DNA. Previous studies showed that polyplexes made by using Lipofectin, a liposomal based transfection agent, also allowed significant PicoGreen intercalation.[29] This technique was used again here to show quantitatively the different steric arrangement of DNA in the knot polyplexes (Figure 2d). Polymer alone controls were also performed to ensure there was no intercalation between SYBR Safe/PicoGreen and the polymers (SI Figure S8), and nuclease degradation studies indicated that the DNA was well protected while in the polyplex form (SI Figure S7).

Transfection and Cytotoxicity Analysis. The transfection capability of the knot polymers was assessed by two different methods, using the secreted G-luciferase protein assay and the cytoplasmic GFP protein analysis by flow cytometry. In each G-luciferase study, the optimum weight ratio is plotted (polymer/plasmid ratios of 3:1 and 5:1 were used for PDE-8% PEG and PDE-14%PEG respectively), with the subsequent effect on cell viability of that weight ratio also being plotted.

The alamarBlue reagent was used to measure any reduction in cell metabolic activity, normalized to indicate cell viability by

dx.doi.org/10.1021/ja2105575 | J. Am. Chem. Soc. 2012, 134, 4782–4789

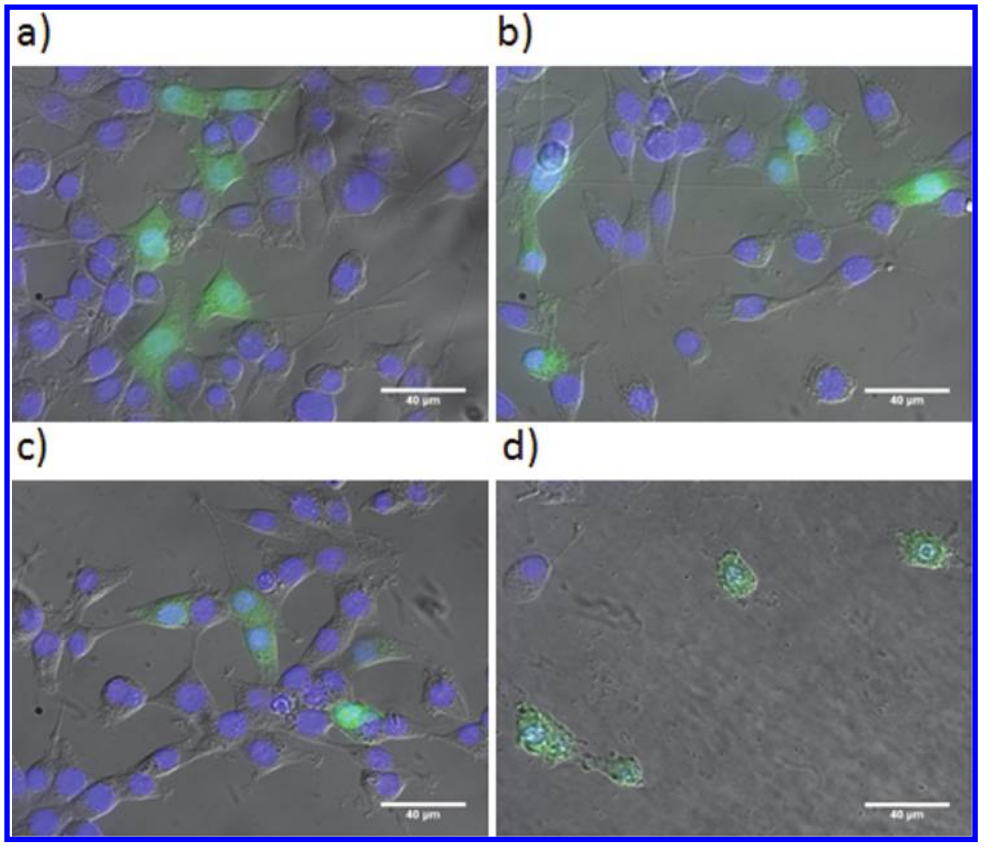

Figure 5. Fluorescent microscopy images of 3T3 cells incubated for 48 h with GFP polyplexes comprised of (a) PD-E 8%PEG, (b) PD-E 14%PEG, (c) PAMAM, and (d) PEI. The nuclear stain DAPI, the cytoplasmic GFP expression, and the brightfield images are overlaid to give a visual representation of individual cell expression.

plotting as a percentage of the control cells. To compare the predominantly cyclized polymer with a highly branched dendrimer structure, the SuperFect PAMAM dendrimer was used as the positive control throughout these studies according to the manufacturers protocol (a polymer/plasmid weight ratio of 8:1). Also, when this PAMAM dendrimer was compared with other commonly used polymer transfection agents (PEI, poly-L-lysine (PLL) and PDMAEMA) it showed a good combination of high transfection and low cytotoxicity (see SI Figure S5), thus providing a strong platform from which to compare the cyclized structure. However, it must be noted here that although SuperFect is a PAMAM dendrimer, the exact generation or chemical structure is not divulged, hence our need to use the weight/weight polymer/plasmid ratio throughout this work for a truly accurate comparison.

Parts a and b of Figure 3 show the effect of changing the degree of PEGylation within these polymer structures. This study showed that PD-E 8%PEG and PD-E 14%PEG exhibited far higher transfection capabilities than did the PD-E 0%PEG and PD-E 20%PEG polymers. Contributing factors likely to promote this trend may be the higher cytotoxicity associated with PD-E 0%PEG, and that past a certain degree of PEGylation, further addition renders the polymer less effective through hindered plasmid/polymer interaction or reduced cell internalization,[30] possibly the case with PD-E 20%PEG (see SI Figure S6). Other preliminary studies had also confirmed this trend held true in other cell lines, so only PD-E 8%PEG and PD-E 14%PEG were taken forward for subsequent studies. The effect of changing the molecular weight was then observed through the synthesis of four PD-E 8%PEG polymers (4, 10, 22, and 30 kDa) followed by analysis with HeLa cells (Figure 3c,d). Despite the low molecular weight polymers showing no toxicity over the weight ratios analyzed, they generally showed a lower transfection capability than the higher molecular weight counterparts, which only showed toxicity at the higher weight ratios. It was therefore decided to use 30 kDa PD-E 8%PEG and PD-E 14%PEG at low polymer/plasmid weight ratios for the analysis over a range of cell types. Immortalized cell lines (3T3, HEK293, and HeLa), primary cells (adipose derived stem cells (ADSC) and nucleus pulposus cells (NP)), and nerve growth factor (NGF) differentiated rat pheochromocytoma (PC12) cells were used to illustrate the potential effectiveness of this structure for a range of different biomedical applications. In four of the cell types PD-E 8%PEG exhibited a significantly higher transfection capability ($P < 0.05$) than did dPAMAM, with only lower transfection in ADSCs (Figure 4). In general, there was little difference in cell viability with both knot polymers, but both cyclic polymers caused significantly lower cytotoxicity than dPAMAM for four of the cell types, with often profound differences being shown. To assess the percentage of cells that were transfected, 3T3 fibroblasts were transfected with the GFP plasmid in either 4/8 well chamber slides for fluorescent microscopy imaging or 6-well plates for flow cytometric analysis. Figure 5 shows qualitatively that large areas of cells can be transfected with widespread GFP expression throughout the cell cytoplasm when PD-E8%PEG is used as the transfection agent. It is interesting to note here that PEI produced only a few (as many were killed), but highly GFP expressing cells. The relatively high transfection values often quoted for PEI are analyzed with secreted proteins, as

dx.doi.org/10.1021/ja2105575 | J. Am. Chem. Soc. 2012, 134, 4782−4789

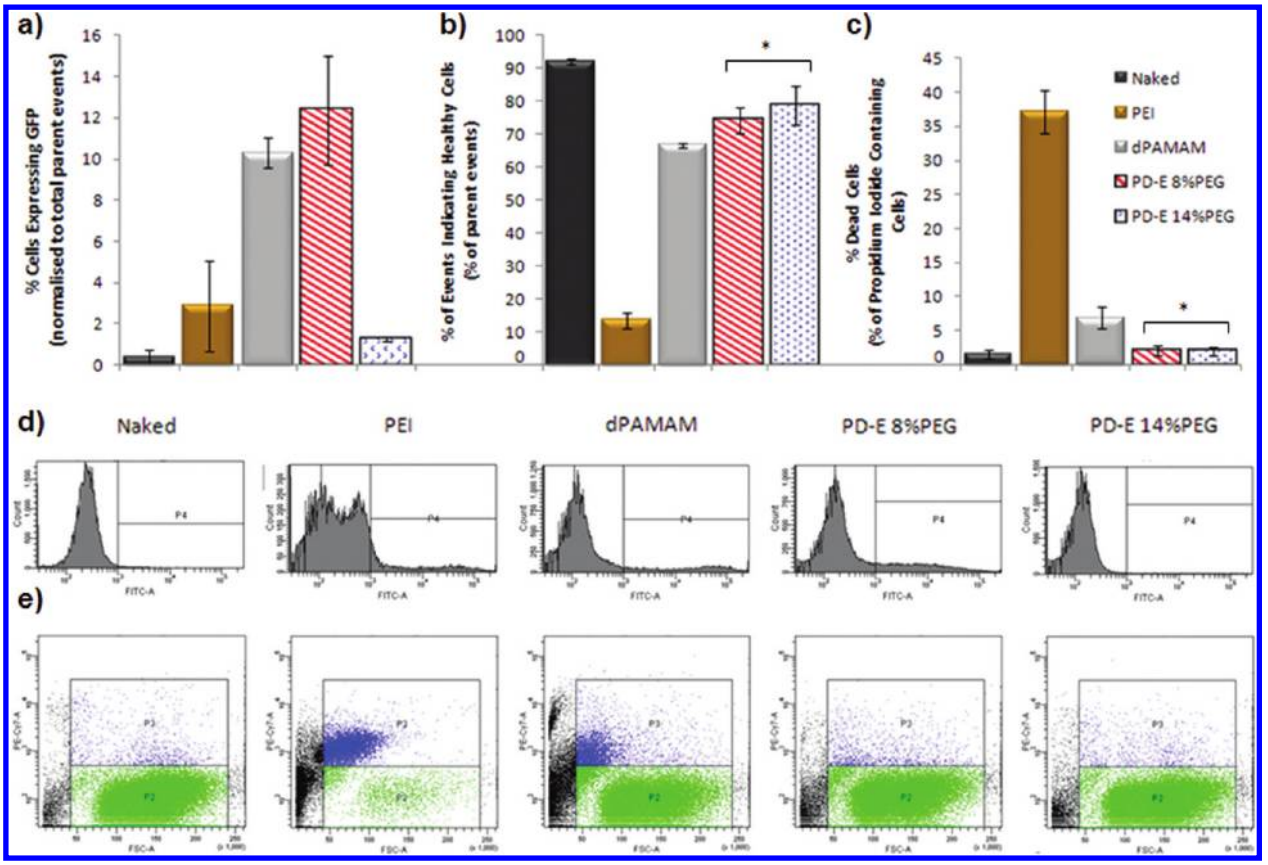

Figure 6. Flow cytometric analysis of GFP expression (a), analysis of cell morphology (b), and propidium iodide (PI) uptake (c) in 3T3 fibroblasts showing that a large decrease in the percentage of parental events occurred with PEI polyplexes is in accordance with an increase in PI fluorescence indicating a large decrease in viability (n = 3, error bars indicate ± standard deviation, asterisk indicates significant difference from dPAMAM). The percentage of total events expressing GFP is highest for PD-E 8%PEG with representative histograms of GFP (FITC) shown in part d. Panel e shows the scatterplots of PI (PE-Cy7A) against forward scatter signal, showing a marked change in morphology and PI uptake for PEI and dPAMAM.

seen in SI Figure S5 (G Luciferase). In this case, few cells can produce significant amounts of the marker protein to be secreted, not so useful for therapies where high numbers of specific cells need transfecting for internally expressed proteins. Figure 6 shows quantitatively that 13% percent of cells expressed GFP when the PD-E 8%PEG vector was used. To obtain this value, null treatment cells were analyzed allowing selection of a gated area of the side scatter signal vs forward scatter signal. This area is termed "normal parent events", i.e. indicative of healthy control cells, where cell debris and polyplex aggregates outside of the gate are ignored. Then the test cells are passed through the FITC filter (GFP) and PE-Cy7A filter (PI), counting cells expressing GFP as a total number of parent events. Although there is no significant increase in PD-E 8%PEG transfection efficiency over dPAMAM, it shows reduced cytotoxicity both in terms of percentage of counting events that fall within the normal parent event area, and in terms of propidium iodide uptake.

Analysis of luciferase expression time showed that both PD-E 8%PEG and PD-E 14%PEG were capable of facilitating transgene expression for 7 days (maximum time tested) with very little decrease in luciferase activity occurring over this period (SI Figure S11). Further to that, the transfection using these polymers was not significantly affected by following the same experimental paradigm in serum conditions (10% FBS) (SI Figure S12). The combination of G-luciferase and GFP data indicates that the knot structured polymers perform generally better than the currently available optimized PAMAM dendrimer, over a range of cell types.

■ CONCLUSIONS

A new cyclic knot polymer structure consisting of single cyclized chain molecules was analyzed in comparison to commercially available transfection agents, in particular with the dendrimer structure of SuperFect (partially degraded PAMAM). This structure of cyclizing chains offers a different pattern of interaction between the polymer and plasmid DNA, and leads to a general profile of higher transfection capability than dPAMAM. By adjusting the monomer ratio of PEG, lower toxicity is also achieved, thus rendering the PD-E8%PEG a more attractive alternative to the PAMAM dendrimer. This study shows only one such set of monomers used in this facile "one-pot" polymerization (in situ DE-ATRP), allowing the possibility for a multitude of variations of knot polymer transfection agents. These cyclized structures, previously unachievable theoretically and experimentally, will open new avenues for the field of gene delivery.

■ ASSOCIATED CONTENT

Ⓢ Supporting Information

GPC traces, ^{1}H NMR spectroscopy of PD-E 8%PEG, PD-E 14%PEG, and disulfide polymer, calculation of degree of branching, transfection studies: comparison of commercial

dx.doi.org/10.1021/ja2105575 | J. Am. Chem. Soc. 2012, 134, 4782–4789

polymers, time course, and effect of serum. This material is available free of charge via the Internet at http://pubs.acs.org.

AUTHOR INFORMATION

Corresponding Author

*wenxin.wang@nuigalway.ie; abhay.pandit@nuigalway.ie

Author Contributions

‡These authors contributed equally to the work

Notes

The authors declare no competing financial interest.

ACKNOWLEDGMENTS

The authors acknowledge Prof. R. Ceredig for flow cytometry assistance and the Science Foundation of Ireland, Strategic Research Cluster (SRC) (grant no. 07/SRC/B1163), Health Research Board (HRB) of Ireland, and Science Foundation Ireland (SFI), SFI Principal Investigator program for financial support of this research.

REFERENCES

(1) Thomas, C. E.; Ehrhardt, A.; Kay, M. A. *Nat. Rev. Genet.* **2003**, *4*, 346−358.
(2) Ansorge, S.; Henry, O.; Kamen, A. *Biochem. Eng. J.* **2010**, *48*, 362−377.
(3) Park, T. G.; Jeong, J. H.; Kim, S. W. *Adv. Drug Delivery Rev.* **2006**, *58*, 467−486.
(4) Putnam, D. *Nat. Mater.* **2006**, *5*, 439−451.
(5) Boussif, O.; Lezoualc'h, F.; Zanta, M. A.; Mergny, M. D.; Scherman, D.; Demeneix, B.; Behr, J. P. *Proc. Natl. Acad. Sci.* **1995**, *92*, 7297−7301.
(6) Haensler, J.; Szoka, F. C. *Bioconjugate Chem.* **1993**, *4*, 372−379.
(7) Yang, C.; Li, H.; Goh, S. H.; Li, J. *Biomaterials* **2007**, *28*, 3245−3254.
(8) Liu, Y.; Nguyen, J.; Steele, T.; Merkel, O.; Kissel, T. *Polymer* **2009**, *50*, 3895−3904.
(9) Zintchenko, A.; Philipp, A.; Dehshahri, A.; Wagner, E. *Bioconjugate Chem.* **2008**, *19*, 1448−1455.
(10) Männistö, M.; Vanderkerken, S.; Toncheva, V.; Elomaa, M.; Ruponen, M.; Schacht, E.; Urtti, A. *J. Controlled Release* **2002**, *83*, 169−182.
(11) Georgiou, T. K.; Phylactou, L. A.; Patrickios, C. S. *Biomacromolecules* **2006**, *7*, 3505−3512.
(12) Xu, F. J.; Zhang, Z. X.; Ping, Y.; Li, J.; Kang, E. T.; Neoh, K. G. *Biomacromolecules* **2009**, *10*, 285−293.
(13) Schallon, A.; Jérôme, V.; Walther, A.; Synatschke, C. V.; Müller, A. H. E.; Freitag, R. *React. Funct. Polym.* **2010**, *70*, 1−10.
(14) Wang, W.; Zheng, Y.; Roberts, E.; Duxbury, C. J.; Ding, L.; Irvine, D. J.; Howdle, S. M. *Macromolecules* **2007**, *40*, 7184−7194.
(15) Newland, B.; Tai, H.; Zheng, Y.; Velasco, D.; Di Luca, A.; Howdle, S. M.; Alexander, C.; Wang, W.; Pandit, A. *Chem. Commun.* **2010**, *46*, 4698−4700.
(16) Flory, P. J. *J. Am. Chem. Soc.* **1941**, *63*, 3083−3090.
(17) Flory, P. J. *J. Am. Chem. Soc.* **1941**, *63*, 3091−3096.
(18) Flory, P. J. *J. Am. Chem. Soc.* **1941**, *63*, 3096−3100.
(19) Stockmayer, W. H.; Jacobson, H. *J. Chem. Phys.* **1943**, *11*, 393−393.
(20) Stockmayer, W. H. *J. Chem. Phys.* **1944**, *12*, 125−131.
(21) Stockmayer, W. H. *J. Chem. Phys.* **1943**, *11*, 45−55.
(22) Zheng, Y.; Cao, H.; Newland, B.; Dong, Y.; Pandit, A.; Wang, W. *J. Am. Chem. Soc.* **2011**, *133*, 13130−13137.
(23) Inoue, K. *Prog. Polym. Sci.* **2000**, *25*, 453−571.
(24) Kim, Y. H. *J. Polym. Sci. Part A: Polym. Chem.* **1998**, *36*, 1685−1698.
(25) Li, Y.; Armes, S. P. *Macromolecules* **2005**, *38*, 8155−8162.
(26) Funhoff, A. M.; van Nostrum, C. F.; Koning, G. A.; Schuurmans-Nieuwenbroek, N. M. E.; Crommelin, D. J. A.; Hennink, W. E. *Biomacromolecules* **2003**, *5*, 32−39.
(27) Varkouhi, A. K.; Scholte, M.; Storm, G.; Haisma, H. J. *J. Controlled Release* **2010**, *151*, 220−228.
(28) Kim, T.-i.; Seo, H. J.; Choi, J. S.; Jang, H.-S.; Baek, J.-u.; Kim, K.; Park, J.-S. *Biomacromolecules* **2004**, *5*, 2487−2492.
(29) Holladay, C.; Keeney, M.; Newland, B.; Mathew, A.; Wang, W.; Pandit, A. *Nanoscale* **2010**, *2*, 2718−2723.
(30) Malek, A.; Czubayko, F.; Aigner, A. *J. Drug Targeting* **2008**, *16*, 124−139.